



ISSN NO. 2320-5407

Journal homepage: <http://www.journalijar.com>

INTERNATIONAL JOURNAL
OF ADVANCED RESEARCH

RESEARCH ARTICLE

Fabrication, Characterization and Adsorption Studies of carbon nanotubes synthesis from camphor reinforced with poly N- methyl aniline.

S. M. Sayyah⁽¹⁾, Amina A.Attia⁽²⁾, Nady A.Fathy⁽²⁾, Mona A.Shouman⁽²⁾, Amgad B.Khalil⁽¹⁾, Khadiga M.Abas⁽²⁾.

1. Polymer Research Laboratory, Chemistry Department, Faculty of Science, Beni Suf University 62514 Beni-Suef, Egypt.
2. Physical Chemistry Department, Laboratory of Surface Chemistry and Catalysis, National Research Center, Dokki, Cairo 12622, Egypt.

Manuscript Info

Manuscript History:

Received: 10 July 2015

Final Accepted: 22 August 2015

Published Online: September 2015

Key words:

MWCNTs, P-NMA, Camphor, C.V.D, Adsorption.

*Corresponding Author

S. M. Sayyah

Abstract

In the present study, multi walled carbon nanotubes (MWCNTs) were successfully synthesized over Ferric nitrate supported on alumina at 850⁰C under a nitrogen flow. Camphor was used as a carbon source which is an environment –friendly agricultural hydrocarbon via chemical vapor deposition (CVD). The as grown MWCNTs combined with polymer (N-methyl aniline) via oxidative dispersion polymerization using ammonium peroxy disulfate (oxidant) in the presence of HCl (dopant). The synthesized materials were characterized by BET, XRD, FTIR, UVVIS, elemental analysis and HRTEM. The application of this synthesized materials were investigated in determination of lead ions in aqueous solution. MWCNTs/(PNMA) "nanocomposite" was found to exhibit the best adsorption capacity (147.3mg/g) indicating that this sorbent possess a great potential application prospect for removing Pb+2 from aqueous solutions. Freundlich model was more suitable to simulate the lead adsorption isotherms than Langmuir model.

Copy Right, IJAR, 2015., All rights reserved

INTRODUCTION

Carbon nanotubes (CNTs) have attracted much interest from researchers owing to their unique structure and physicochemical properties. CNTs have been constructed with high length-to-diameter ratio, significantly larger than that of any other material, giving them outstanding electronic, mechanical and thermal properties [1,2]. Because of their high surface area and large micropore volume, CNTs are also considered as extremely good adsorbents [3]. Among several techniques of CNTs synthesis available today, chemical vapor deposition (CVD) is the most popular and widely used because of its low set-up cost, high production yield, and ease of scale-up.

Most commonly used CNTs precursors are petroleum products [4,5,6]. Considering the environmental effects and declining petroleum product sources, efforts are now directed to switch over to reproducible natural carbon sources. Our effort is mainly focused on identifying and using regenerative, environmentally, clean and inexpensive natural products as precursors for the synthesis of CNTs. It is found that camphor is a white crystalline bicyclic saturated ketone with a characteristic pungent odor and taste that is flammable and volatile, it readily ignites and burns without producing any residues. Camphor [C₁₀H₁₆O] is carbon-rich, hydrogen rich, and oxygen present, also it consists of both sp² and sp³ carbons, it is an attractive new material for carbon-based preparation, since graphite has only sp² carbon [7,8]. Because of very low catalyst requirement with camphor, as-grown CNTs are least contaminated with metal, whereas oxygen atom present in camphor helps in oxidizing amorphous carbon in-situ. These features of camphor stimulated more in depth, basic an applied research world wide. Additionally, the catalyst is the key factor for CNT growth in CVD reactor. Most commonly-used metals are Fe, Co, Ni, because of two main reasons: (i) high solubility of carbon in these metals at high temperatures and (ii) high carbon diffusion rate in these

metals [9,10]. Metal-substrate reaction (chemical-bond formation) would cease the catalytic behavior of the metal. Alumina materials are reported to be a better catalyst support owing to the strong metal-support interaction, which allows high metal dispersion and thus a high density of catalytic sites.

However, the insolubility and weak dispersibility of CNTs in common solvents and matrices have limited their application. An effective method used to improve the dispersion of nanotubes is the modification of CNTs by polymers. Intrinsically conductive polymers (ICP_s) are organic polymers that conduct electricity. Electrical conductivity of conducting polymers can be tuned from insulating to metallic through proper doping. They have a conjugated structure with alternate σ and π bonds. The π bonds are delocalized throughout the entire polymer network. This results enhanced electrical conductivity [11]. Example of conducting polymer that has been commonly used in nanocomposite fabrication is polyaniline, which is commonly prepared by in-situ polymerization in which the monomer is chemically oxidized in the presence of the filler [12]. Polyaniline is a prototype conducting polymer, it is particularly attractive for electric applications due to its facile synthesis, environment stability, unique electronic properties, and simple acid/base doping/dedoping chemistry [13]. In situ polymerization is one of the most important methods developed so far to incorporate the dopant in poly aniline during synthesis. A great variety of organic and inorganic dopant acids can be used, such as hydrochloric acid, sulfuric, nitric, perchloric, tartaric, camphorsulfonic and 4-toluenesulfonic acid.

In this work, we attempted to synthesize CNTs by the catalytic decomposition of camphor [an eco-friendly] natural carbon source using iron catalyst supported on alumina by CVD method. The produced CNTs reinforced with the oxidative chemical polymerization of N-methyl aniline in aqueous HCl and ammonium peroxy disulfate as an oxidant. Also XRD, TEM, SEM, FTIR and BET analysis techniques were used to fully characterized the materials. The obtained nanomaterials were tested towards the removal of lead (II) from aqueous solution.

2-Experimental

2.1. Materials

All the reagents used in the study were of analytical and used as received without any further purification grade obtained from Merck and Fluka. Ferric nitrate $\text{Fe}(\text{NO}_3)_3 \cdot 9\text{H}_2\text{O}$, Aluminum hydroxide $\text{Al}(\text{OH})_3$, Ammonium peroxy disulfate $(\text{NH}_4)_2\text{S}_2\text{O}_8$, Hydrochloric acid (HCl), and finally camphor $\text{C}_{10}\text{H}_{16}\text{O}$, which was obtained locally. N-methyl aniline was vacuum distilled before use. The physical properties of camphor and N-methyl aniline is given in table (1).

2.2. Synthesis of Oxide Catalyst

Catalyst was prepared by dissolving the right amount of iron (III) nitrate nanohydrate in double distilled water and followed by impregnation onto the $\text{Al}(\text{OH})_3$ supports with 5 wt % of metal catalyst. Metal impregnated catalyst sample was dried at 100°C over night and calcined in air at 700°C for 3 h.

2.3. Synthesis of CNTs

2.2. Synthesis of Oxide Catalyst

Catalyst was prepared by dissolving the right amount of iron (III) nitrate nanohydrate in double distilled water and followed by impregnation onto the $\text{Al}(\text{OH})_3$ supports with 5 wt % of metal catalyst. Metal impregnated catalyst sample was dried at 100°C over night and calcined in air at 700°C for 3 h.

2.3. Synthesis of CNTs

The synthesis of CNTs was carried out in cylindrical furnaces the first one for evaporating camphor at 250°C , and the second one for depositing the vapors over the catalyst at 850°C in a nitrogen atmosphere at a flow rate of 50 ml/min. The reaction was kept under these conditions for 30 min. After the reaction, the furnace was cooled to room temperature in a nitrogen flow. The carbon samples, in black powder form were collected from the tube reactor for purification. The as grown CNTs were purified through reflux in nitric acid and hydrochloric acid (5M) for 4 h at 100°C . Then, precipitate was washed and dried over night at 100°C (MWCNTs).

2.4. Synthesis of poly N-methyl aniline and poly N-methyl aniline /CNTs nanocomposite

Poly N-methyl aniline is prepared using oxidative aqueous polymerization. The oxidative polymerization reaction was performed in a well-stoppered conical flask of 250 ml at room temperature. A desired amount of N-methyl aniline 0.55 ml (0.1M) was added into 25 ml HCl (0.1M) under stirring. Ammonium peroxy disulfate (oxidant) was dissolved in distilled water (25 ml) and then added to the reaction mixture. This solution is kept in shaking for 1 h. After 1 h of shaking the polymer is filtered, and dried in an air oven at 60°C (P-NMA).

The CNT/(P-NMA) nanocomposite was prepared by drop wise chemical polymerization method with HCl as dopant and (APS) as an oxidant. A known amount of MWCNTs (0.25 gm) is dispersed in 0.2M (APS) solution. A known amount of monomer N-methyl aniline (0.55 ml) was mixed with 0.1 M HCl, this solution was added drop wise into carbon nanotubes mixture under continuous stirring for 1 h in ultrasonic water bath. The precipitate was

filtered, washed and dried under vacuum at 60°C MWCNTs/(P-NMA) nanocomposite. The weight ratio of CNTs: monomer was (0.5:1)

2.5. Characterization of Nanomaterials

- 1] The infrared spectroscopy measurements were performed (FTIR-6100 Jasco Spectrophotometer to identify the functional groups of the nanomaterials).
- 2] The microstructure and morphology of the materials were observed with JEM-2100 (JEOL-ELECTRON MICROSCOPE).
- 3] Surface area and porosity were defined by nitrogen adsorption isotherms of the materials (Quanta Chrome NOVA Automated GAS Sorption System Version 1.12).
- 4] The X-ray diffraction analysis of the samples is carried out using a fully automated Rigaker 1710 X-ray diffractometer. In our set-up filtered Cu-K₂ radiation having wave length 1.542 Å is used for diffraction . The accelerating potential applied to the X-ray tube is 30 KV and the tube current is 20 mA.
- 5] For the chemical characterization of carbon materials, carbon, hydrogen ,and nitrogen analysis is performed. They are determined automatically by Vario microanalyzer system.
- 6] The ultraviolet-visible absorption spectra of the prepared polymer was measured using Shimadzu UV-VIZ spectrophotometer at room temperature in the range (350-900 nm) using dimethyl formamide as a solvent and reference.

2.6. Adsorption Studies

The adsorption studies of lead by the nanomaterials were studied by the batch equilibrium method. A stock solution was obtained by dissolving 1.6 gm of Pb(NO₃)₂ in 1 L to get concentration of 1000 (mg/L) by using distilled water. An atomic absorption apparatus of the type (Perkin Elmer model 2380 A.A.S) was employed to determine the lead content in the treated solutions after carrying the necessary dilutions to conform the desired levels of the metal.

Batch equilibrium data were carried out by contacting 10 mg of nanomaterials with 10 ml of Pb(NO₃)₂ solution containing Pb⁺² ions of varying concentrations (20-100 mg/L) at PH=6. The stoppered bottles were shaken well for 24 h.

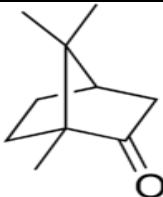
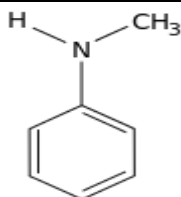
The amount of absorbed Pb⁺² (mg/g) was calculated based on a mass balance equation as given by equation (1):

$$q_e = (C_0 - C_e)V/W \rightarrow (1)$$

Where q_e is the equilibrium adsorption capacity gram dry weight of the adsorbent (mg/g), C₀ is the initial concentration of Pb⁺² in the solution (mg/L), C_e is the final equilibrium concentration of Pb⁺² in the solution (mg/L), V is the volume of the solution (L), and W is the weight of nanomaterials (mg).

3- Results and discussion

Table (1): Physical Properties of Camphor and N-methyl aniline

Name	Camphor	N-methyl aniline
Molecular structure		
IUPAC name	1,7,7-Trimethylbicyclo[2.2.1]heptan-2-one	N-methyl aniline
Molecular formula	C ₁₀ H ₁₆ O	C ₇ H ₉ N
Molar mass	152.23 g.mol ⁻¹	107.15306 g.mol ⁻¹
Density	0.992 g .cm ⁻¹	0.999 gm.cm ⁻¹
Melting point	175°C (374°F ; 448°K)	-57°C (-71°F ; 216°K)

3.1. Infrared Spectrum (FTIR)

Figure (1) shows the FTIR spectra of the polymer, fabricated CNTs and the nanocomposite, the related peaks are summarized in table (2). Only a small C-C stretch and a peak at 1514 cm^{-1} to 1541 cm^{-1} were observed, which indicates the presence of a carbon double bond C=C; this finding confirms the hexagonal structure of the CNTs [14]. Strong bands are evident in the region $(1498-1743)\text{ cm}^{-1}$ which may be due to C=C in CNTs and stretching vibration of C=C in benzene ring or C=N in the quinoid ring for the polymer [15]. Very weak and broad band around 3000 cm^{-1} is assigned to N-H stretching mode. The N-H stretching region near 3000 cm^{-1} showed strong and broad peaks. The interaction between the MWCNTs and (P-NMA) may result in charge transfer, resulting a decrease in the N-H stretching intensity. The bands due to C=O are very prominently seen in the range $(1685-1831)\text{ cm}^{-1}$ for both CNTs and nanocomposite which can be assigned to the acid-carbonyl stretching mode. Other bands seen in all samples are small one in the range at $(2856-2924)\text{ cm}^{-1}$ that are characteristic of C-H of MWCNTs or N-H symmetric stretching vibration in polymer. The bands at 3434 cm^{-1} representative to O-H for MWCNTs, this shift in this band to 3445 cm^{-1} indicates the change in the MWCNTs structure upon polymerization [16].

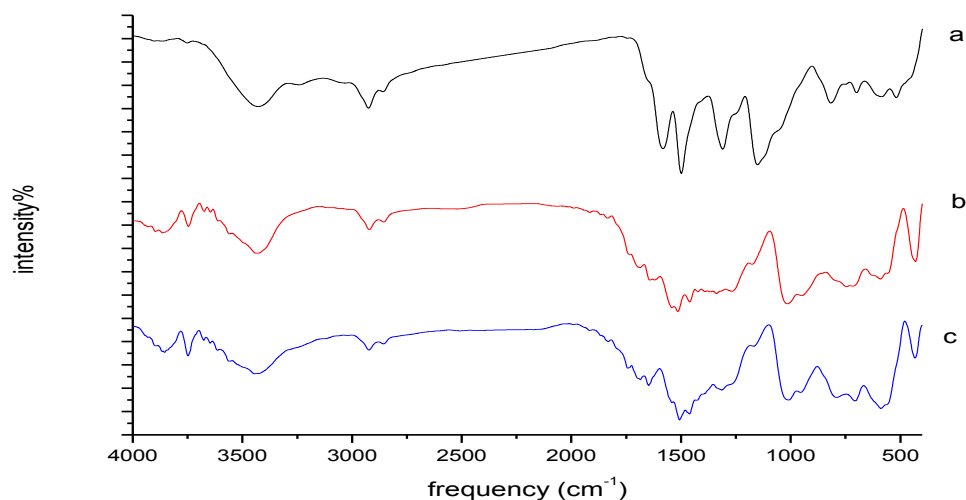


Figure (1): FTIR of the tested nanomaterials

a) P-NMA b) MWCNTs c)MWCNTs/(P-NMA) nanocomposite

3.2. The XRD analysis

The XRD pattern: figure (2) of CNTs sample revealed the presence of two peaks at 26.5° and 43.4° corresponding to the interlayer spacing (0.34 nm) of the nanotube (d_{002}) and the (d_{100}) reflection of the carbon atoms, respectively, in good agreement with the literature [17]. The asymmetry of the band at 43.4° was due to the turbostratic nature of the nanotubes. However XRD for the polymer and MWCNTs/(P-NMA) (nanocomposite) are completely amorphous [18].

Whereas, XRD pattern for the catalyst, displays that all diffraction peaks were perfectly indexed to the XRD pattern of pure boehmite (JCPDS card 1-083-2384) indicating that the boehmite exhibited excellent crystallinity and a high purity [19].

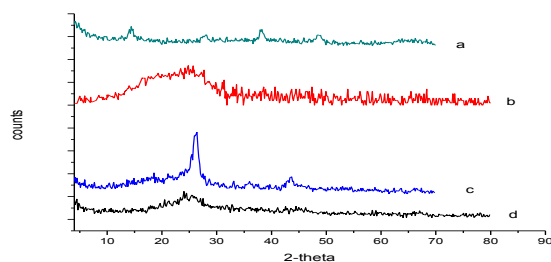


Figure (2): XRD of the tested nanomaterials

(a) catalyst (b) (P-NMA) (c) MWCNT (d) nanocomposite

Table (2): FTIR spectroscopy absorption bands of tested nanomaterials.

Frequency(cm^{-1})			Assignments
CNTs/ Fe at 700 ⁰ c	CNTs/ (P-NMA) nanocomposite	(P-NMA)	
-----	555.398 ^w	518.758 ^b	Bending deformation of N-H group attached to benzene ring
-----	589.147 ^b	586.254 ^{v.b}	
-----	705.819 ^b	700.034 ^b	Out of plane C-H deformation of 1,4-disubstituted benzene ring in polymer
-----	789.707 ^b	746.317 ^w	
-----	-----	816.706 ^b	
-----	-----	1047.16 ^{sh}	
-----	-----	1151.29 ^b	
950.734 ^b 1.015.34 ^b	955.555 ^b 1010.52 ^b	-----	O-H bending in CNTs
1175.41 ^b	1169.62 ^b	-----	Prove that the band observed at about 1700 cm^{-1} is due to carboxylic group
1267.97 ^b	1269.9 ^{sh}	-----	C-O stretching for CNTs and symmetric stretching vibration for C-O or C-N for polymer
-----	-----	1243.86 ^{sh} 1310.39 ^s	
1459.85 ^m	1461.78 ^b	-----	C-H stretching
1514.81 ^m	-----	-----	C=O carbonyl group in CNTs
1541.81 ^w	1507.1 ^s 1541.81 ^w	-----	
-----	1647.88 ^s	-----	Due to C=C in CNTs and stretching vibration of C=C in benzene ring or C=N in quinoid unite for polymer
1642.09 ^w	1742.37 ^b	1498.42 ^s 1582.31 ^m 1743.33 ^w	
-----	-----	-----	
1685.48 ^b	1685.48 ^w	-----	Can be attributed to ester group or carboxylic group
1685.48 ^b 1833.97 ^b	1685.48 ^w 1831.08 ^b	-----	Due to C=O
2856.06 ^b 2921.63 ^b	2856.06 ^b 2922.59 ^b	2858.95 ^b 2924.52 ^m	Due to C-H stretching of CNTs or N-H symmetric stretching vibration in polymer
-----	3022.87 ^w	3032.51 ^b 3242.72 ^b	Stretching vibration of C-H aromatic for polymer structure
-----	-----	3426.89 ^{st,b}	Asymmetric stretching vibration of N-H in polymer and O-H stretching for CNTs
3434.6 ^b	3445.21 ^b	-----	
-----	-----	3752.8 ^b	Stretching vibration of O-H group

3.3. High resolution transmission electron microscope (HRTEM)

HRTEM micrograph of (P-NMA), MWCNTs and MWCNTs/(P-NMA) nanocomposite are shown in Figure (3). These micrograph figures (3,a,b) show that (P-NMA) exist as spherical beads or ellipsoidal particles varied sizes ranging from 1 μm to 2 μm , either separated or linked with each other. Figure (3,c) shows HRSEM micrograph of MWCNTs without purification reveals the formation of abundance of carbon nanotubes which are forest like. While after purification figure (3,d), the image suggests that the MWCNTs have smooth, clean and straight surfaces with diameter ranging from 200-500 nm, with outer diameter in the range 116.24 nm and internal diameter of about 32.67 nm and their lengths ranging in several microns. MWCNTs/ (P-NMA) composites figure (3,e) shows the homogeneous coating of polymer onto the CNTs indicating that CNTs were well dispersed in polymer matrix. Nanocomposite shows well aligned and elongated structure with diameter ranging from 100-500 nm, with internal diameter of about 22.24 nm and outer diameter of about 39.07 nm, and thickness is about 3.56 nm whereas the length of about 1 μm [20].

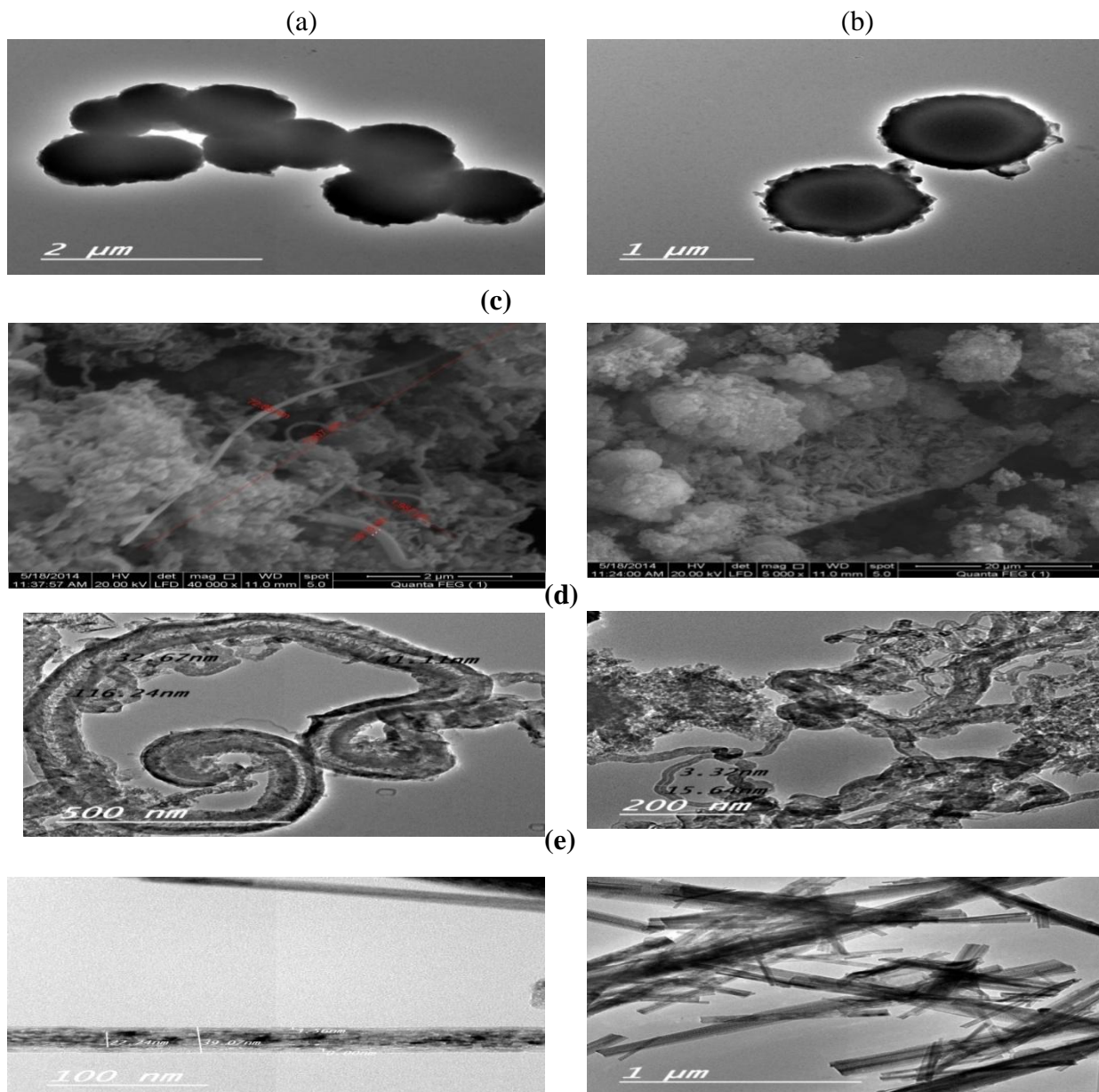


Figure (3): HRTEM of (P-NMA) (a,b) , MWCNTs before purification (c), after purification (d), MWCNTs / (P-NMA) nanocomposite (e).

3.4. Surface Area Analysis

Detailed information on the textural properties of the nanomaterials is listed in table (3). As shown there was drastically change in the texture characteristics, as it was associated with the reduction in all parameters of the internal porosity. The high specific surface area provides large number of sorption sites to aniline monomer which can polymerize to form coating over the nanotubes. After the incorporation of polymer into the matrix of MWCNTs, the BET surface area of nanocomposite decrease to 146.5 m²/g. In addition the pore volume also decrease without significant change in the pore diameter of the nanocomposite. This, it further supports the conjecture, that polymer covers and coats inside and outside the surface of MWCNTs [21], larger the surface area greater will be the number of reducing groups hence more attributed to better MWCNTs sorption performance. But according to our results, the efficient removable of the lead ions was strongly associated with the functional groups which is present onto the surface [22].

Table (3): Textural properties of the tested nanomaterials

	(P-NMA)	MWCNTs	CNTs/(P-NMA) nanocomposite
Surface area(m ² /g)	48.72	207.2	146.5
Total pore volume(cm ³ /g)	0.02	0.1052	0.0745
Average pore diameter (A ⁰)	16.5	20.32	20.34

3.5. Elemental analysis

Previous studies showed that the molecular weight of (P-NMA) can be substantially increased by the oxidative polymerization of NMA with ammonium peroxy disulphate. The real mass proportions of (P-NMA), MWCNTs and MWCNTs/(P-NMA) nanocomposite respectively were determined using elemental analysis and compared with nominal compositions in table (4). It is revealed that the molecular weight of MWCNTs increased after polymerization with N-methyl aniline in nanocomposite.

Table (4) : Elemental analysis of the tested nanomaterials

Sample name	N%		C%		S%		Cl%	
	Calculated	Found	Calculated	Found	Calculated	Found	Calculated	Found
(P-NMA)	10.4	10.64	62.39	62.36	11.88	19.72	6.59	6.44
CNT/Fe at 700 ⁰ c	Found	0.803	Found	63.27	Found	0.024	Found	0.76
Nano composite (CNTs/ (P-NMA))	Found	3.747	Found	70.46	Found	0.66	Found	5.33

3.6. Determination of the optimum polymerization conditions

To optimize the conditions for polymerization of N-methyl aniline, the concentrations of ammonium peroxy disulfate, hydrochloric acid and monomer were investigated with keeping the total volume of the reaction medium constant at 50 ml.

3.6.1. Effect of ammonium peroxy disulfate concentration

Both of the monomer and HCl concentrations were kept constant at 0.1 M and 0.2 M respectively while the oxidant concentrations were varied from 0.05 to 0.7 M to investigate the optimum polymerization condition of (NH₄)₂ S₂ O₈. It is obvious from figure (4,a), that the yield increased with the increase of (NH₄)₂S₂ O₈ reaching a maximum value at 0.2 M. This is interpreted on the fact the produced initiator ion radical moieties that activate the backbone and simultaneously produce the N-methyl aniline ion radical. However a decrease was noticed beyond this concentration. This is due to a high concentration of the oxidation which promotes the formation of low molecular weight oxidation product. This leads to a degradation in the produced polymer which is easily soluble in water.

3.6.2. Effect of N-methyl aniline concentration

The effect of monomer concentration on the polymerization yield was investigated in the range of monomer concentrations from 0.04 to 0.3 M and the data was represented in figure (4,b). It is revealed from Figure (4,b) that, the optimum yield formation is obtained at 0.1 M of the monomer concentration.

3.6.3. Effect of HCl concentration

Oxidative chemical polymerization of substituted-aniline can occur within a very wide interval range of acidity. Polymerization in basic, neutral and weakly acidic media gives brown powder while in highly acidic medium conducting dark-green emeraldine can be obtained. As revealed from figure (4,c) the yield increase by increasing the acid concentration from 0.02 M to 0.1 M then gradually decreases up to 0.5 M. This can be explained on the basis that increasing the concentration led to the degradation of the polymer in the early stages, due to hydrolysis of polyemeraldine chain.

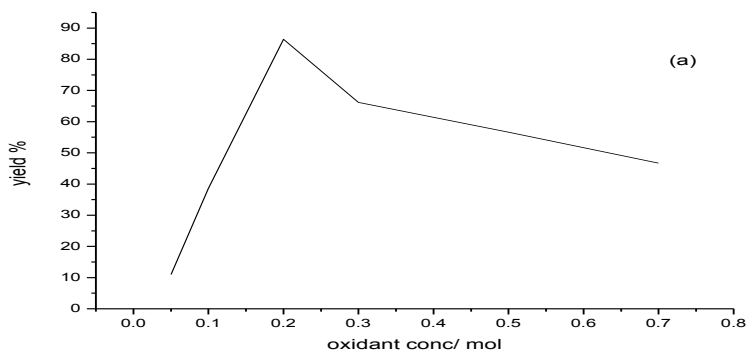
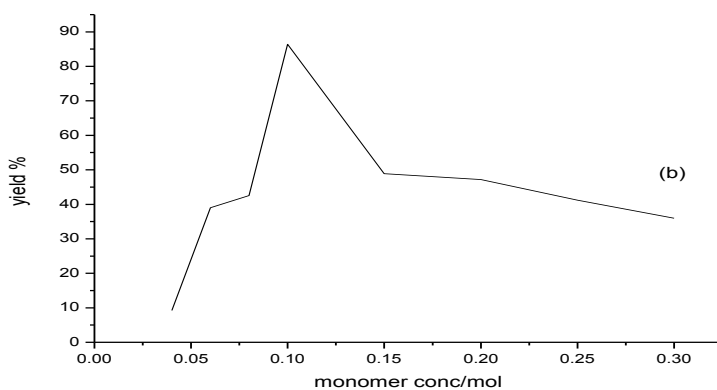
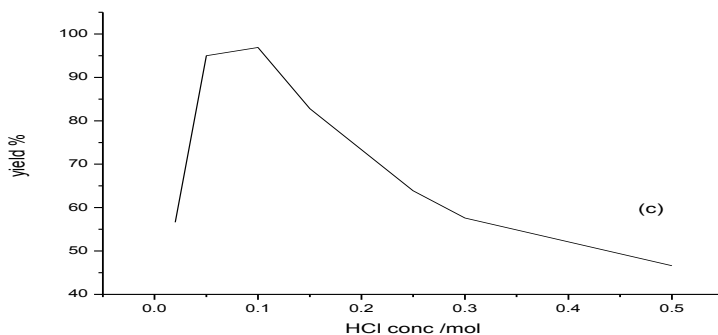


Figure (4,a)-Yield- $(\text{NH}_4)_2\text{S}_2\text{O}_8$ concentration effect on the aqueous oxidative polymerization of N-methyl aniline.



Figure(4,b)-Yield-monomer concentration effect on the aqueous oxidative polymerization of N-methyl aniline.



Figure(4,c)-Yield-HCl concentration effect on the aqueous oxidative polymerization of N-methyl aniline.

3.7. Solubility

Polyaniline has low solubility in most polar and non-polar solvents.

The solubility of (P-NMA) was investigated in, dimethylformamide (DMF), acetone, methanol, iso propanol, chloroform and benzene at 25⁰C. The solubility values are listed in table (5), slightly soluble in DMF, acetone, methanol and iso propanol at 25⁰C but insoluble in benzene, and chloroform.

Table (5): Solubility of (P-NMA) in different solvents

Solvent	Solubility of P(NMA)in g/l
DMF	2.3
Acetone	5.8
Methanol	3.4
Isopropanol	3

3.8. The UV-VIS Absorption Analysis

Figure (5) represents the UV-VIS absorption spectra of pure (P-NMA) dispersed in dimethylformamide. The (P-NMA) spectrum revealed a sharp peak at 350 nm, which was assigned to the benzenoid rings due to π - π^* transition in molecular conjugation. A broad peak at approximately 450 nm originated from the charged cationic species called polarons [23].

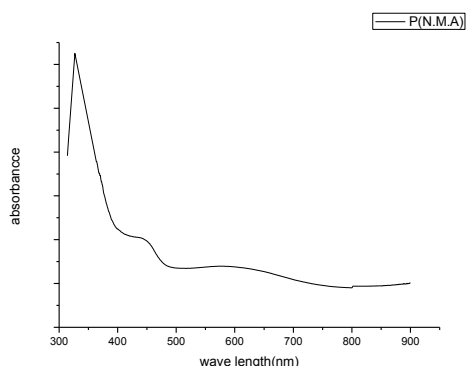


Figure (5): UV-Visible Spectra of the (P-NMA)

3.9. Adsorption Isotherm

The most famous isotherm models that are used to express the distribution of metal ions between solid and liquid phases are Langmuir and Freundlich [24,25]. The main assumption of Langmuir model is presence of mono layer coverage of the adsorbate on the adsorbent surface and there is the same activation energy for adsorption of every molecule on the surface. The Langmuir expression is given by

$$q_e = q_m \cdot K_L C_e / (1 + K_L C_e) \quad \rightarrow \quad (2)$$

Where q_e and q_m are the values of metal ions adsorbed after equilibrium and the saturation capacity of the monolayer, respectively. K_L is the Langmuir constant, which depends on the affinity of binding sites. q_m and K_L are determined from intercept and slope of C_e versus C_e/q_e .

Freundlich isotherm originates from the multilayer adsorption on the heterogeneous surface. This model obeys:

$$q_e = K_F \cdot C_e^{1/n} \quad \rightarrow \quad (3)$$

Where K_F and n are the Freundlich constant, which indicates the capacity and power of adsorption, respectively. The adsorption isotherms are given in figure (6). From the isotherm parameters, table (6) it is evident that modification of MWCNTs by polymer inflects a remarkable effect on the metal removal capacity. It is obvious that at first, the adsorption is relatively rapid while with increase in equilibrium concentration the adsorption is leveled off. As seen in table (6) the correlation coefficient value R^2 obtained shows that the equilibrium data fit better with Freundlich model [26]. This leads to that the surface area of each adsorbent is made of small heterogeneous adsorption patches which are nearly similar to each other in adsorption capacity. It might be inferred that the presence of generated -COOH, on the surface of MWCNTs, also the presence of amine or imine groups in

the polymer intensifies the metal uptake capacity [27,28]. Accordingly, these modification by polymer N-methyl aniline should be highly recommendable for the efficient removal of the metal ions from the metal contaminated effluents with loading up to 100 ppm.

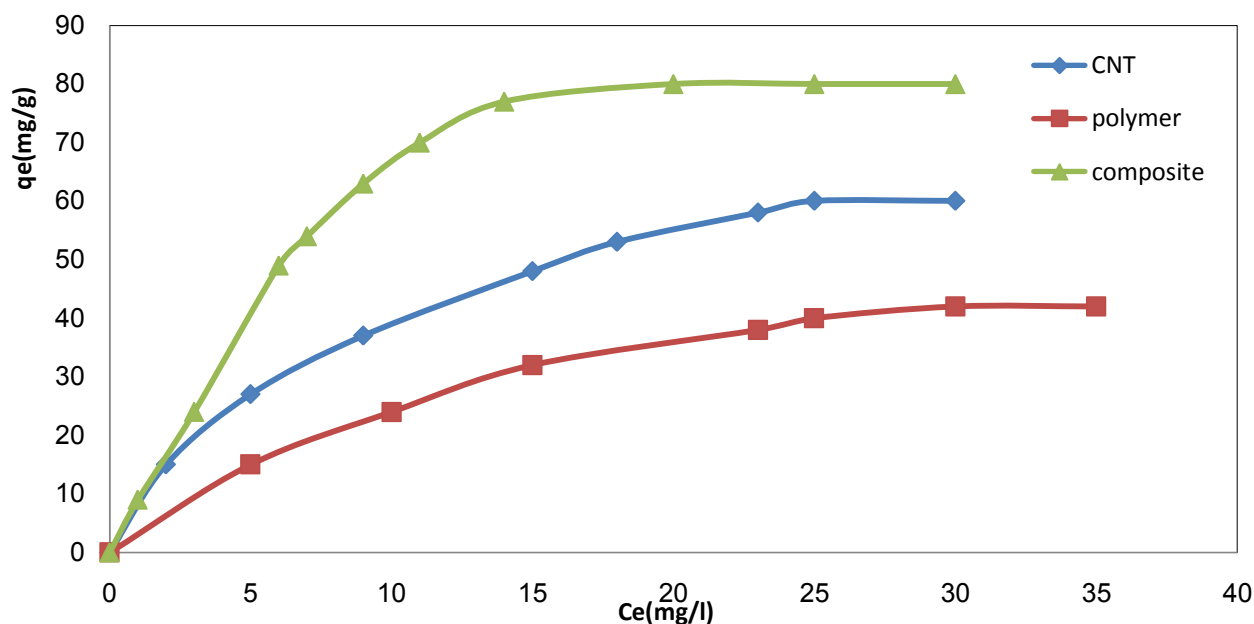


Figure (6): Adsorption isotherm for Pb(II) onto tested nanomaterial

Table (6): Langmuir and Freundlich parameters for Pb⁺² adsorption on tested nanomaterials:

Adsorbent	Langmuir			Freundlich		
	K _L	Q ₀	R ²	K _F	n	R ²
(P-NMA)	0.068	52.5	0.80	14.12	1.73	0.98
MWCNTs	0.052	60	0.82	13.18	2.27	0.97
MWCNTs/(P-NMA)nanocomposite	0.135	147.3	0.81	19.95	1.92	0.99

Conclusions

In summary, MWCNTs have been synthesized using camphor as a carbon source via chemical vapor deposition. The catalyst obtained by impregnation method, contained 5wt% of iron nitrate supported on alumina. The boehmite phase which appears in the XRD patterns for the catalyst seems to be involved in enhancing the activity of iron ions in the production of MWCNTs. The optimum yield formation of (P-NMA) is obtained by using 0.2 M ammonium peroxy disulfate, 0.1 M of monomer and 0.1M of HCl. FTIR spectra confirmed the hexagonal structure of CNTs because of the presence of a peak corresponding to the carbon double bond. HRTEM images of the synthesized materials showed the formation of MWCNTs and incorporation of (P-NMA) inside and outside the surface of nanotubes. The sorption mechanism of lead onto synthesized materials depends mainly on the chemical interaction between the lead ions and the surface functional groups. The maximum adsorption capacity of MWCNTs/ (P-NMA) nanocomposite was found to be 147.3 mg/g. Furthermore, the adsorption isotherms are well described by the Freundlich equation.

4- References

- 1] Iijima S. Helical microtubules of graphitic carbon *Nature*, 354, 56 (1991) doi:10.1038/354056aO.
- 2] Ajayan PM, Stephan O, Colliex C, Trauth D. Aligned carbon nanotube arrays formed by cutting a polymer resin-nanotube composite *Science*, 265, 1212 (1994). doi: 10.1126/science.265.5176.1212
- 3] R.Q.Long and R.T.Yang, Carbon nanotubes as superior sorbent for dioxin removal. *J. of American Chemical society* 123, 9, 2058-2059, 2001.
- 4] Jay bhaye SV, Sharon M, Singh LN, Study of hydrogen adsorption by spiral carbon nanofibers synthesized from acetylene. *Synthetic React. Inorg. Metal–Org. Nano-Metal Chem*, 36, 37 (2006).
- 5] B. Q. Wei, R.Vajtai, Y.Jung, J.Ward, R.Zhang, G. Ramanath, P. M. Ajayan. Microfabrication technology: Organized assembly of carbon nanotube *Nature* 416, 495 (2002).
- 6] B.C.Satishkumar, A. Govindaraj, C.N.R, Rao. Bundles of aligned carbon nanotubes obtained by the pyrolysis of ferrocene-hydrocarbon mixture, role of metal nanoparticles produced in situ, *Chem. Physical Letter*, 307, 158 (1999).
- 7] M. Kumar, T. Okazaki, M. Hiramatsu, Y. Ando. The use of camphor-grown carbon nanotube array as an efficient field emitter. 45, 1899 (2007).
- 8] S. Maruyama, R. Kojima, Y. Miyauchi, S. Chiashi, M. Kohno. Low-temperature synthesis of high-purity single-walled carbon nanotubes from alcohol, *Chem.Phys. Letter*, 360, 229 (2002).
- 9] Murakami Y, Miyauchi Y, Chiashi S, Maruyama S. Characterization of single-walled carbon nanotubes catalytically synthesized from alcohol. *Chem. Phys. Lett.* 374, 53 (2003).
- 10] N. Nagaraju, A. Fonseca, Z. Konya, J. B. Nagy. Alumina and silica supported metal catalysts for the production of carbon nanotubes, *J. Mol, Catal. A*, 181, 57 (2002).
- 11] David I Bower, An introduction to polymer physics, Cambridge – University Press, Cambridge, 2002.
- 12] Gangopadhyay, R, De, A, Conducting polymer nanocomposites a brief overview. *Chem.Mater.* 2000, 121, 608-622.
- 13] D.Li, J.X.Huang, R.B.Kaner, Poly aniline nanofibers a unique polymer nanostructure for versatile applications. *Accounts Of Chemical Research.* 42, 135-145, 2009.
- 14] R. Yudianti, H. Onggo, Y. Saito, T. Iwata, and J.I. Azuma, "Analysis of functional group sited on multi walled carbon Nanotube Surface" *Open Materials Science Journal*, 5, 242-247 (2011).
- 15] S.Quillard; G Louran; S Lefrant; A.G MacDiamid. Vibrational analysis of polyaniline: A comparative study of leucoemeraldine, emeraldine, and pernigraniline bases. *Phy. Rev. B*, 1994, 50, 17, 12496.
- 16] Said M Sayyah, Ahmed A. Aboud, Amgad B. Khaliel, Salma M. Mohamed. Oxidative Chemical Polymerization of O-tolidine in acid medium using $K_2Cr_2O_7$ as oxidizing agent and characterization of the obtained polymer. *Int. J. of advanced Research*, 2, 6, 586-607.
- 17] V. S. Angulakshmi, S.Karthikeyan, P. S. Syed Shabudeen. Effect of synthesis temperature on the growth of multi walled carbon nanotubes from ZEAMAYS oil as evidenced by structural, RAMAN and XRD analysis. *RASA'YAN. J. Chem.* 8, 1, 1-7, 2015.
- 18] M. Wan and J. Li " Microtubules of poly aniline doped with HCl and HBF_4 " *J. of Polymer Science A*, 37, 4605-4609 (1999).
- 19] Jing Yang, Rayl. Frost Synthesis and Characterization of Boehmite Nanofibers. *Research Letters in Inorganic Chemistry* ID 602198, doi: 10.1155/2008/602198 (2008).
- 20] Sarika Mishra, Anoop Kumar S, AvanishPratap Singh, A. C. Nigam. Comformally Poly aniline coated Multi Walled carbon nanotubes: Synthesis and Characterization. *Chemistry*, 5, 5, ISSN-2249-555X (2015).
- 21] Rami Regueira, Ran Yosef Suckeveriene, Irena Brook, Gry Mechrez, Roza Tchoudakov, Moshe Narkis. Investigation of the electro-mechanical behavior of hybride Poly aniline/Graphene nanocomposites Fabricated by Dynamic Interfacial Inverse emulsion Polymerization. *Graphene*, 4, 7-19 (2015).
- 22] NadyA.Fathy, Amina A. Attia. Bahira Hegazi, Nanostructured activated carbon xerogels for removal of methomyl pesticide Desalination and water treatment (2015) 1-14 doi: 10. 1080/19443994. 2015. 1032362
- 23] Van Hao Nguyen, Jae-Jin Shim "Green Synthesis and Characterization of Carbon nanotubes / Poly aniline Nanocomposite. *J. of Spectroscopy.* Article ID 297804, (2015).
- 24] C.H.Wu, "Studies of the Equilibrium and Thermodynamics of the adsorption of Cu^{+2} onto As-produced and modified carbon Nanotubes " *J. of colloidal and Interface Science*, 311, 2, 338-346 (2007).
- 25] C. Chen, X.Wang. Adsorption of Ni (II) from aqueous solution using oxidized multi walled carbon nanotubes. *"Industrial and Engineering Chemistery Research*, 45, 26, 9144-9149 (2006).
- 26] M. S. Mansour, M. E. Ossman, H. A. Farag. Removal of Cd (II) ion from waste by adsorption onto poly aniline coated on saw dust. *Desalination* 272, 301-305 (2011).

- 27] R. Ansari, F. Raofie. Removal of Lead Ion from aqueous solution Using Saw dust Coated by poly aniline E-Journal of Chemistry, 3, 1, 49-59, (2006).
- 28] Sayyah, S. M. and Abd El Salam, H. (2006). Oxidative Chemical Polymerization of Some 3-alkyloxyaniline Surfactants and Characterization of the Obtained Polymers. Int. J. Polym. Mater. 55: 1075-1093.